CFSRC COLLOQUIUM

Proceedings of the Cold-Formed Steel Research Consortium Colloquium
20-22 October 2020 (cfsrc.org)

Compression Tests of Fixed Ended CFS Members with Improved Connectors

Son Tung Vy[1], Mahen Mahendran[2]

Abstract

In the compression tests of cold-formed steel (CFS) members, fixed end supports are commonly simulated by fixing the test specimens to end plates by either welding or casting them with high strength adhesives. This is costly, time consuming and takes much effort to ensure that the axial compression loading is applied correctly. Some past research studies have used clamping connectors for this purpose, but had many limitations relating to their flexibility in use and restraining capacity. This research study has used an improved clamping connector system to provide fixed end support conditions in the compression tests of CFS members, which can be easily adjusted to suit different CFS sections. A series of compression tests using the new clamping connector system was conducted on single channels, built-up back-to-back channels and nested (box) channels with their lengths in the range of 0.6 to 3.0 m. Test results were then analyzed and compared with corresponding finite element analyses based on ideal fixed end support conditions. Comparison of results showed the suitability of the new clamping connector system to simulate fixed end supports.

1. Introduction

Cold-formed steel (CFS) compression members have been increasingly used in building construction. Their popular applications are columns in CFS portal frames, truss members, studs in light gauge steel frames and storage racks. Recently, they are also used as wall studs in mid-rise buildings. Although many past research studies have been conducted on these members, further research studies are continuing to provide more comprehensive understanding and knowledge on their behavior and to develop advanced design rules.

In the research studies of CFS compression members, experimental study is an important step since it provides valuable data for developing validated numerical models and design methods. In general, the test procedures should follow the standard test methods in ASTM E9-19 [1], which nominates three ideal specimen end support conditions, including pinned-pinned, pinned-fixed and fixed-fixed as shown in Figure 1. However, this standard does not provide any details for setting up these end support conditions. Besides, AISI S902-17 [2] includes the set-up of end supports for CFS compression members, however, it may only be suitable for short members which fail by local buckling. Further, AISI S910-17 [3] only presents the test set-up for CFS hat-shaped compression members failing in distortional buckling mode. In conclusion, none of the current test standards provides the set-up details of end supports for the tests of CFS members with varying lengths, which may fail by either local, distortional, local-global or global buckling.

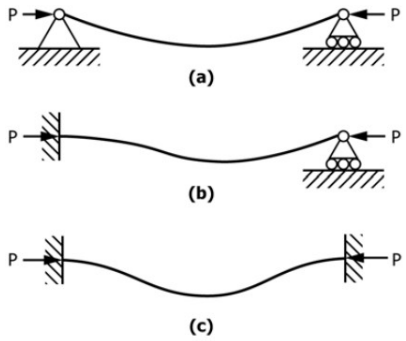

Figure 1: Three ideal end support conditions [1]: (a) pinned-pinned, (b) pinned-fixed and (c) fixed-fixed.

To ensure the ideal fixed-fixed or pinned-pined end support conditions nominated in ASTM E9-19 [1], many research studies have used welded connections [4-8] or high strength adhesive [9-11] to attach the CFS specimen ends to the end loading plates, as shown in Figures 2 (a)-(b). These methods can fully restrain the axial and lateral movements, rotations and warping of the specimen ends, thus, the above ideal end support conditions can be ensured. However,

[1] PhD researcher, Queensland University of Technology (QUT), Australia, sontung.vy@hdr.qut.edu.au
Lecturer, National University of Civil Engineering (NUCE), Vietnam
[2] Professor, Queensland University of Technology (QUT), Australia, m.mahendran@qut.edu.au

using welded connections may affect the material properties and imperfections of the test specimen, while the adhesives requires long curing time to achieve acceptable strength. Besides, both these methods are expensive due to the costs of adhesive and welding, temporary support system for the specimens before using adhesive or welding, weld installation and large number of non-reusable end loading plates. Further, using these methods, it is difficult to ensure that the axial compression loading is applied correctly, especially for long compression members.

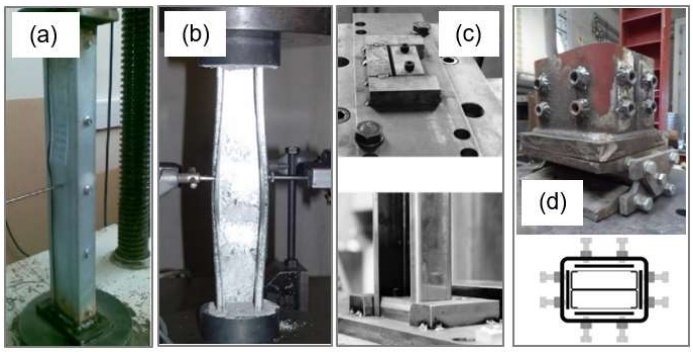

Figure 2: Test set-up in some past research studies.

Some research studies [12-14] have used clamping connectors for tests of fixed ended CFS compression members, as shown in Figure 2 (c). The weakness of these connectors is that they were specially designed for only one type of section shape with specific dimensions. Besides, Craveiro [15] used a more complex clamping connector system shown in Figure 2 (d) for his compression tests of CFS single channel, and built-up back-to-back, boxed and double-boxed channel members. However, these connectors only provided semi fixed-fixed end supports for the test specimens as shown by the corresponding finite element (FE) models which used the rotation stiffness of the end supports used in the tests to be flexible to obtain good validation.

This paper aims to develop and use an improved connector system which can provide ideal fixed-fixed end supports for CFS compression with many advantages compared with the above-mentioned test methods used in past research studies. Firstly, the design and working mechanism of the improved connectors are briefly presented, followed by a compression test series conducted using the improved connectors on 0.6, 1.5 and 3.0 m long CFS single channel, built-up back-to-back and nested (boxed) channels. Test results were then analyzed and compared with the results from corresponding FE modelling based on ideal fixed-fixed end support conditions. The comparison of test and FE analysis results showed that the new clamping connector system is suitable to simulate fixed-fixed end supports of CFS compression members in test conditions.

2. Design of improved connectors

Figures 3-4 show the details of the connectors used to clamp a single channel (SC) or built-up back-to-back (BC) specimen. Each connector included four 20 mm thick steel side plates welded together, and welded to a 10 mm thick steel end plate to form a box. The end plate was used to stop the axial movement of the specimen's end segment. Besides, there were four fully-threaded M12 bolts (restraining bolts) attached on each steel side plate by threaded nuts (welded to the steel side plate). They supported steel plates F1 and F2, and steel blocks B1 and B2 to prevent the lateral movements, bending and twisting of the specimen's end segment. The thickness of these steel plates was designed as 10 mm while the widths of the steel blocks were controlled as 0.5 to 1 mm smaller than the inner depth of the specimen's cross section to eliminate the effect of gaps between the steel blocks and the specimen's flanges. Since the stiffness of the flange and web elements of the specimen's end segment is negligible compared to that of the steel plates, the steel blocks and the restraining bolts, these elements were fully restrained against lateral movements, bending and twisting. Based on the same mechanism, lips of the specimen's end segment were also restrained by steel plates S1 to S4, which were attached to the steel plates F1 and F2. In conclusion, the end support conditions of the single channel or BC specimen could be considered as fixed.

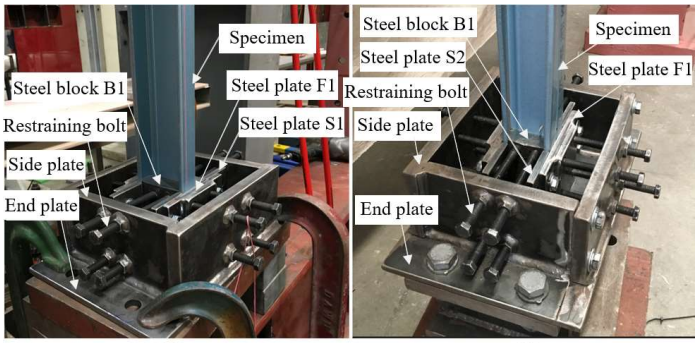

Figure 3: Specimens fixed inside the bottom connector: (a) single channel and (b) BC.

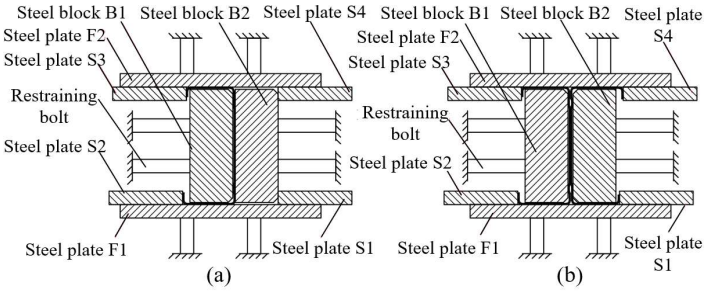

Figure 4: Sketches of specimens fixed inside the bottom connector: (a) single channel and (b) BC.

As shown in Figures 5-6, there were some modifications in

the connector when using it for the built-up nested CFS channel (NC) specimen. Initially, the steel blocks B1 and B2 were relocated to the outside of the specimen section while the steel plates S1 to S4 were removed. Besides, an additional steel block B3 was placed inside the specimen section, between its flanges. This design solution was successful to effectively restrain the overall twisting of the specimen end segment and the lateral movements of its flanges. Furthermore, each web of the specimen's end segment was attached to a corresponding steel block (B1 or B2) through two additional M6 "web bolts". This meant that the webs of the specimen's end segment could be laterally restrained. In conclusion, the end support conditions of the NC specimen could also be considered as fixed.

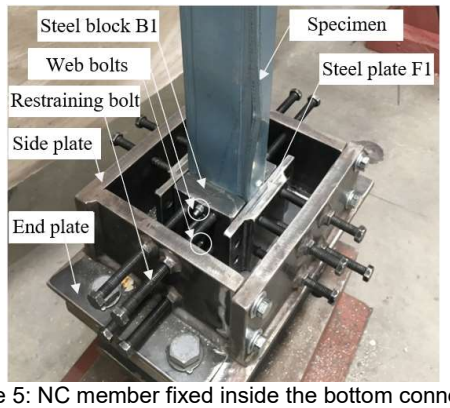

Figure 5: NC member fixed inside the bottom connector.

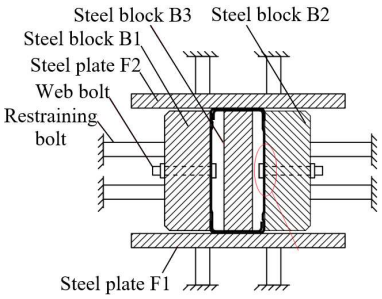

Figure 6: Sketch of NC member fixed inside the bottom connector.

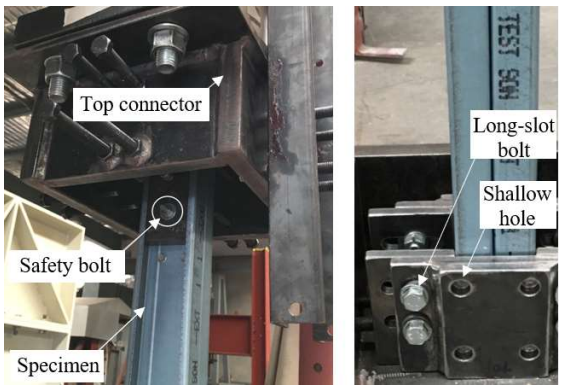

Figure 7: Other details of the connectors.

Some other details of the connectors are also important for the tests. In Figure 7, the steel plates S1 to S4 were connected to the steel plates F1 and F2 by long-slot bolts. Thus, the transverse positions of the steel plates S1 to S4 could be modified to fit different flange widths of specimens. Besides, at the top connector, they were attached to the specimen via a safety bolt M10 to prevent the steel blocks falling-off. Meanwhile, the steel plates F1 and F2 were designed with four shallow holes at the position of the restraining bolts. This also ensured that the restraining bolts could prevent these steel plates from falling-off.

3. Experimental program

3.1. Test specimens

In this test series, a commercially available channel section in Australia was selected for making all the test specimens, including single channel, BC and NC members. This section was made of high strength steel grade G550 (nominal yield strength of 550 MPa) and its average thickness without the zinc-coating layer is 0.95 mm. The sketch of the channel section is shown in Figure 8 (a) while its average measured dimensions are shown in Table 1.

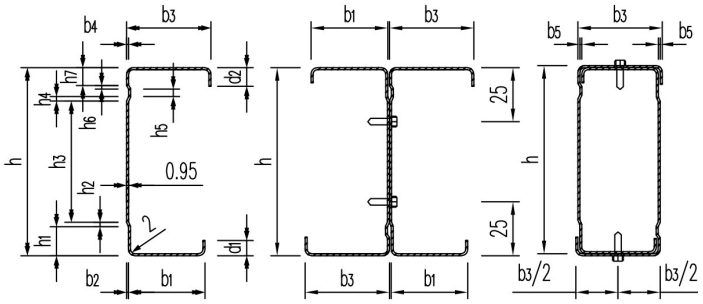

Figure 8: Test specimen cross-sections.

Table 1: Dimensions of the channel section used in tests.

Dimension	Value (mm)	Dimension	Value (mm)
h_1	13.42	b_1	35.71
h_2	2.09	b_2	0.80
h_3	56.24	b_3	39.30
h_4	2.06	b_4	0.89
h_5	3.48	b_5	0.85
h_6	1.62	d_1	7.01
h_7	8.31	d_2	8.63

The specimen lengths were chosen as 800, 1700 and 3200 mm, which were 200 mm greater than their actual lengths used in the calculations and FE models. This was because in the test set-up, both end segments of test specimens were clamped inside the connectors, for 200 mm in total. To limit the length tolerance and the unexpected non-uniform stresses applied to the specimen during the test, each specimen was cut to a pre-specified length and milled flat at both

ends.

To fabricate a BC member or a NC member shown in Figures 8 (b)-(c), two single channel members were connected together along the longitudinal direction by using 10g self-drilling hex-head screws. Their relative positions were adjusted carefully to ensure that the built-up member was doubly-symmetric and its ends were almost flat. Furthermore, based on the recommendations of Li et al. [16], the screw spacings (s) were selected as 150, 300 and 600 mm for BC and NC members with their actual length (L) of 600, 1500 and 3000 mm, respectively.

3.2. Test rig and operations

A typical test set-up is shown in Figures 9-11, where a CFS specimen was vertically compressed under a stable and strong test frame that was fixed to a reinforced concrete strong floor. The 100 mm long bottom end segment of the specimen was fixed inside the bottom connector, attached to a bottom frame beam (for the 600 mm long specimen), or to the floor (for the 1500 or 3000 mm long specimen). Similarly, the 100 mm long top end segment of the specimen was fixed inside another connector, located under a load cell. Connecting to the top of the load cell, a 200 kN hydraulic jack was used to apply the compression load on the specimen through the load cell. The top of the hydraulic jack was fixed to a top beam to ensure that it was kept stable during the test. Furthermore, the axial shortening of the specimen was recorded by a draw-wire displacement sensor, located between the jack and the top connector.

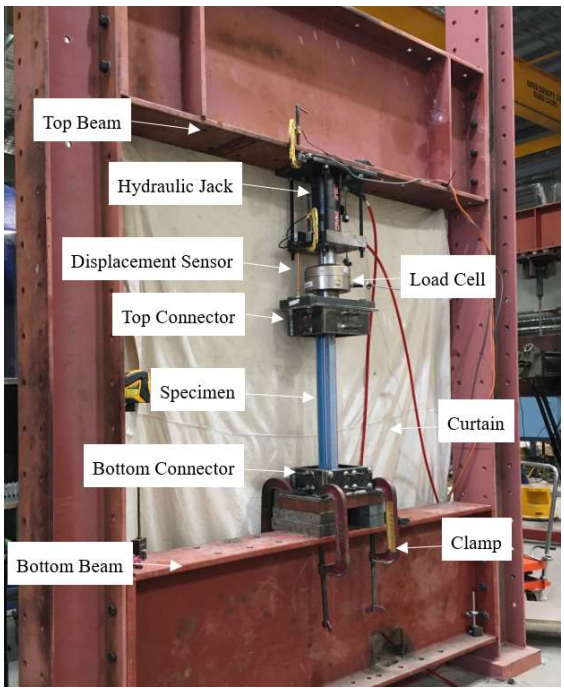

Figure 9: Test set-up for a 600 mm long specimen.

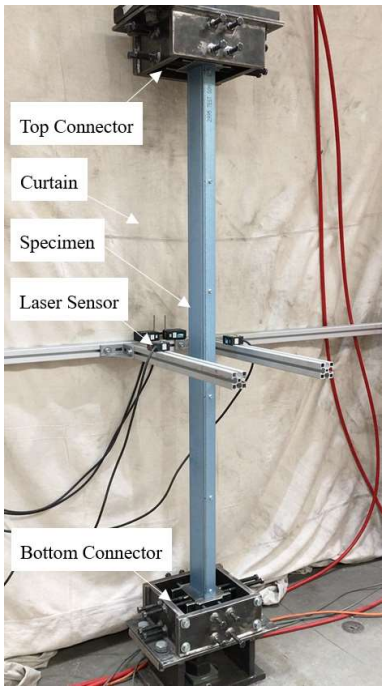

Figure 10: Test set-up for a 1500 mm long specimen.

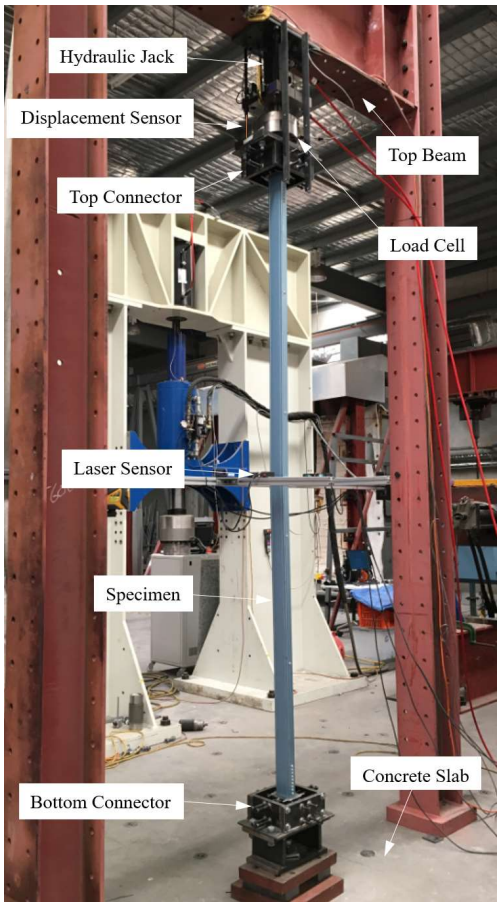

Figure 11: Test set-up for a 3000 mm long specimen.

Before the test, the top and bottom connectors were verified to ensure their end plates' surfaces were level, and their central points and the hydraulic jack's axis were in a vertical line. When the specimen was clamped inside the top and bottom connectors, the length and the compression load of each restraining bolt were adjusted carefully to make the specimen vertical and place in the central points of the connectors' end plates. Its verticality was checked by two line laser levels located in front and on the left side of the test frame. To minimize any gaps between the specimen and the connector's end plate, the hydraulic jack initially applied an axial load of about 3 kN to the specimen, and was then released. Then, the compression test was started when the hydraulic jack applied a load at a rate of 1 mm/min. During the test, a computer program, UDAQ, was used for collecting the data of the applied load and shortening of the specimen every second from the load cell, draw-wire and displacement sensors. The test was terminated when the specimen experienced post-peak failure deformations.

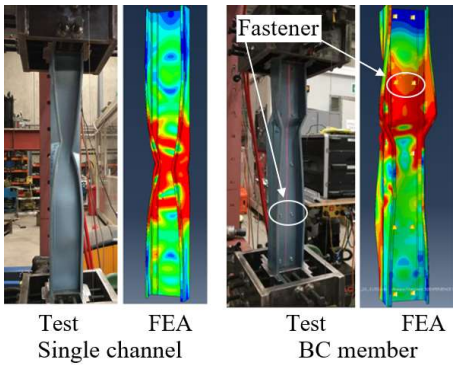

Figure 12: Deformed shapes of 600 mm long specimens.

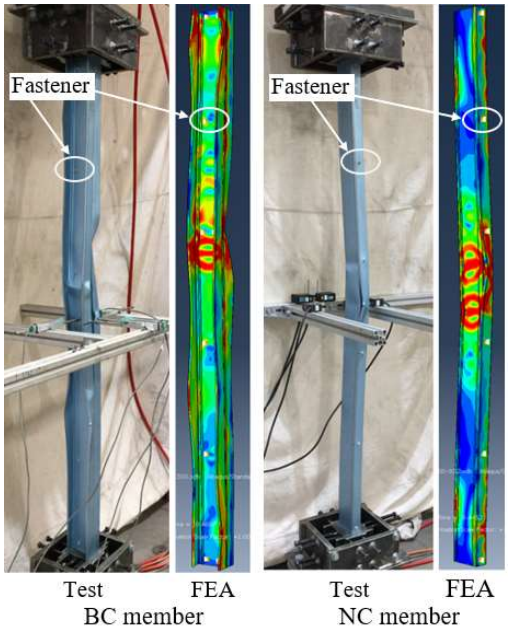

Figure 13: Deformed shapes of 1500 mm long specimens.

3.3. Test results

Figures 12-14 show the deformed shapes of specimens after the tests. Based on the deformed shapes, the failure mode of 600 mm long single channel and BC specimens was considered to be local-distortional interaction buckling as their longitudinal axes remained straight and vertical, while their flanges rotated along the flange-web junction and local buckling deformations occurred at some locations of their webs. When the member length increased, the effect of global buckling was more significant on the compression behavior of specimens. Indeed, 1500 mm long BC and NC specimens failed in the local-flexural interaction buckling mode as they clearly bent about their minor axes and the web local buckling deformations were still observed around mid-length. This buckling mode was also observed in the failures of 3000 mm long BC and NC specimens, however, the effect of flexural buckling was more dominant. In contrast, 3000 mm long single channel specimens were dominated by flexural-torsional buckling failures.

The ultimate loads of all test specimens are summarized in Table 2, while some examples of load versus shortening curves are shown in Figure 15. They have shown that the differences, in terms of the ultimate loads and the pattern and stiffness of load versus shortening curves, between repeated test results of each type of specimen were marginal (less than 5%). This indicates that the test results are reliable and the test set-up using the improved connector system worked well in all the tests of single channel, BC and NC members.

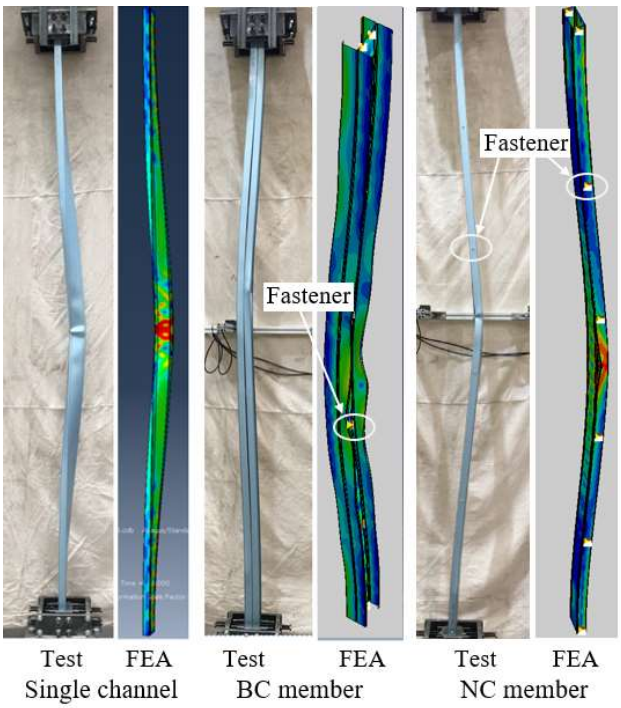

Figure 14: Deformed shapes of 3000 mm long specimens.

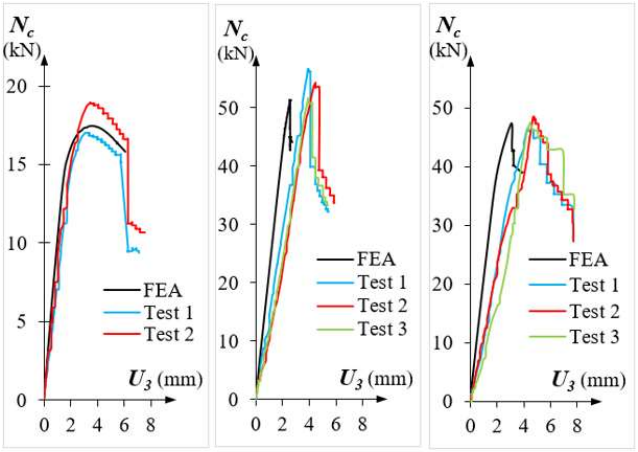

Single channel BC NC

Figure 15: Load versus shortening curves for 3 m long specimens.

Table 2: Comparison of test and FE analysis results.

Specimen	Length (mm)	Test	$N_{c,Test}$ (kN)	$N_{c,FEA}$ (kN)	$N_{c,FEA}$ / $N_{c,Test}$
Single Channel	600	a	46.32	47.20	1.02
Single Channel	600	b	48.89	47.20	0.97
Single Channel	3000	a	17.02	17.46	1.03
Single Channel	3000	b	18.94	17.46	0.92
BC	600	a	95.71	91.39	0.95
BC	600	b	94.04	91.39	0.97
BC	600	c	95.08	91.39	0.96
BC	1500	a	85.90	81.68	0.95
BC	1500	b	85.11	81.68	0.96
BC	3000	a	56.63	51.30	0.91
BC	3000	b	54.34	51.30	0.94
BC	3000	c	51.58	51.30	0.99
NC	1500	a	87.03	90.63	1.04
NC	1500	b	91.33	90.63	0.99
NC	3000	a	46.46	47.25	1.02
NC	3000	b	48.47	47.25	0.97
NC	3000	c	47.46	47.25	1.00
Average					0.98
COV					0.04

4. Finite element modelling

The commercial program Abaqus/ CAE 2019 was used to develop the FE models of the tested CFS single channel, BC and NC members. The FE models included the accurate section geometries (Figure 16) and nonlinear material properties of each specimen. The S4R element was used to model the elements of each member, while a mesh of 5 mm x 5 mm was selected based on a convergence study.

For the case of 600 mm long BC member, which failed by local-distortional interaction buckling, the "general contact" with "hard contact" normal behavior was included to ensure no surface overlapping between their individual (channel) members. However, for the 1500 or 3000 mm long BC and NC members, which were more dominated by global buckling failures, the "surface-to-surface contact" with the same normal behavior was applied to reduce the processing time while the surface overlapping problems were also prevented. Following the assumptions of Phan and Rasmussen [17], each screw fastener in a built-up CFS member was modelled by a Abaqus's point-based fastener linking the coupling points together. The point-based fastener incorporated the shear load versus in-plane displacement relationship as backbone curves, between the corresponding coupling points on the screwed surfaces in FE models. Further, the required backbone curves were determined by using the proposal of Phan and Rasmussen [18] with the elastic modulus (E) and thickness (t) of steel plates, and the screw diameter (d) of the test specimens.

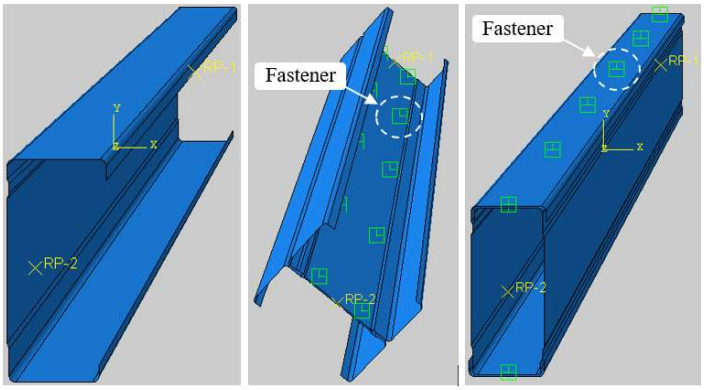

(a) Single channel (b) BC (c) NC

Figure 16: FE models of test specimens.

To include the effect of initial geometric imperfections, eigenvalue buckling analyses of single channel and built-up members (including "contacts") were conducted first. Based on their first global and local buckling modes, as shown in Figure 17, the initial geometric imperfections were incorporated in the nonlinear FE models. In case global buckling mode was not obtained from the eigenvalue buckling analyzes, the section thicknesses were increased so that global buckling became the first buckling mode. Additionally, the magnitude of global imperfections was selected as 1/2000 of the member length while that of local imperfections followed the recommendation in AS/NZS 4600 [19].

To prove that the new connectors are suitable for providing the ideal fixed-fixed end supports for the tested CFS members, the corresponding end support boundary conditions were applied in all FE models of single channel, BC and NC members investigated in this study. Initially, by using MPC type TIE, their end cross sections were constrained to a reference point (RP-1 or RP-2), located at the centroids of the end cross sections. All the axial and lateral displacements (U_x, U_y and U_z) and rotations (UR_x, UR_y and UR_z) of the bottom reference point (RP-1) were restrained. Meanwhile, the top reference point (RP-2) was set similarly except releasing the axial displacement (U_z). Displacement control was used

to apply the axial compression load via RP-2.

Finally, because of the complexity of the section geometry and contacts in each BC or NC member, the Static/General solver was applied where the specific damping factor was 0.0005 and the maximum ratio of stabilization was 0.005.

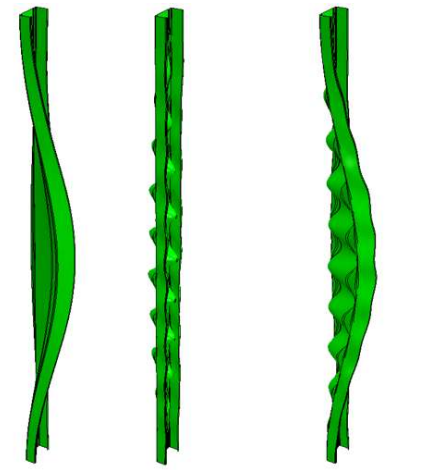

Figure 17: Imperfections incorporated in FE models of channels.

5. Comparison of test and finite element analysis results

The test and FE analysis results were compared based on the failure modes, load versus shortening curves and ultimate loads. Figures 12-14 exhibit good similarities between the deformed shapes of specimens observed in tests and FE analyses. They also show that the failure modes predicted by FE analyses are similar to those observed in the tests. As shown in Table 2, the ultimate loads predicted by FE analyses agree well with those from tests with the average ratio of FE analysis predictions to test results of 0.98 and COV of 0.04. In Fig. 15, the patterns of the load versus shortening curves from the tests and FE analyses are the same. However, the stiffnesses of the load versus shortening curves from FE analyses were higher than those from test results. The reasons for this are considered to be (1) modelling only the clear length of 600, 1500 or 3000 mm, (2) additional local bearing deformations of the clamped segments and (3) localized imperfections and variations along the specimen length. Overall, the predictions of FE models for the compression behavior and capacity of single channel, BC and NC specimens were similar to those from the tests using the improved connector system. As the end support boundary conditions of CFS members in FE models were set as ideal fixed-fixed, the improved connector system was considered to be suitable in providing fixed-fixed end supports for the CFS compression members in tests.

6. Conclusions and discussions

This paper has proposed an improved clamping connector system for CFS compression member testing and described its design and working mechanism. A compression test series using this system was conducted on CFS single channel, BC and NC members with varying lengths, followed by developing corresponding finite element models based on ideal fixed ended support boundary conditions. The test results were shown to be reliable while the good agreement observed between test and FE analysis results showed that the improved connector system is suitable to provide fixed end support conditions for CFS compression members.

The improved connectors also provide the following advantages: (1) shortening the time used for test installation and dismantling to within an hour for each test), (2) ensuring the correct application of the axial compression loading, even for long CFS columns, (3) flexible applications for different cross sections and (4) reusable. In this paper, the improved connectors were only used for ambient temperature tests of CFS compression members. However, with their proven capabilities, they can also be used in more complex tests of CFS members such as compression tests at elevated temperatures and tests under combined axial and lateral loading.

7. Acknowledgments

The authors would like to thank QUT, Australian Research Council (Grant Number LP170100951), National Association of Steel Framed Housing (NASH) and Stoddart Group for providing financial support, research facilities and test materials, and Banyo Laboratory Technical staff for their assistance during the tests. The first author appreciates the assistance of Mr. Ngoc Hieu Pham and Mr. Dang Khoa Phan from the University of Sydney, and Mr. Thananjayan Sivaprakasam from QUT in relation to screw shear tests and nonlinear FE analyses.

References

[1] ASTM E9-19, Standard Test Methods of Compression Testing of Metallic Materials at Room Temperature. Pennsylvania, U.S.A: ASTM, 2019.

[2] AISI S902-17, Test Standard for Determining the Effective Area of Cold-Formed Steel Compression Members, 2017 Edition. Washington, DC, U.S.A.: AISI, 2018.

[3] AISI S910-17, Test Standard for Determining the Distortional Buckling Strength of Cold-Formed Steel Hat-Shaped Compression Members, 2017 Edition. Washington, DC, U.S.A.: AISI, 2018.

[4] S.F. Nie, T.H. Zhou, Y. Zhang, B. Liu, Compressive

behavior of built-up closed box section columns consisting of two cold-formed steel channels, Thin Wall Struct 151, 2020.

[5] K. Roy, T.C.H. Ting, H.H. Lau, J.B.P. Lim, Experimental and numerical investigations on the axial capacity of cold-formed steel built-up box sections, J Constr Steel Res 160, 2019.

[6] E.S. Santos, E.M. Batista, D. Camotim, Experimental investigation concerning lipped channel columns undergoing local–distortional–global buckling mode interaction, Thin Wall Struct 54, 2012.

[7] B. Young, J. Chen, Design of cold-formed steel built-up closed sections with intermediate stiffeners, J Struct Eng 134(5), 2008.

[8] J.H. Zhang, B. Young, Experimental investigation of cold-formed steel built-up closed section columns with web stiffeners, J Constr Steel Res 147, 2018.

[9] S. Gunalan, M. Mahendran, Improved design rules for fixed ended cold-formed steel columns subject to flexural–torsional buckling, Thin Wall Struct 73, 2013.

[10] Y.B. Kwon, B.S. Kim, G.J. Hancock, Compression tests of high strength cold-formed steel channels with buckling interaction, J Constr Steel Res 65, 2009.

[11] T. Ranawaka, M. Mahendran, Distortional buckling tests of cold-formed steel compression members at elevated temperatures, J Constr Steel Res 65, 2009.

[12] B. Rossi, J.P. Jaspart, K.J.R. Rasmussen, Combined Distortional and Overall Flexural-Torsional Buckling of Cold-Formed Stainless Steel Sections: Experimental Investigations, J Struct Eng 136(4), 2010.

[13] L. Zhang, K.H. Tan, O. Zhao, Experimental and numerical studies of fixed-ended cold-formed stainless steel equal-leg angle section columns, Eng Struct 184, 2019.

[14] M. Rokilan, M. Mahendran, Behaviour of cold-formed steel compression members at sub-zero temperatures, J Constr Steel Res 172, 2020.

[15] H.D. Craveiro, Fire resistance of cold-formed steel columns (Ph.D. Thesis), University of Coimbra, Coimbra, Portugal, 2015.

[16] Y.Q. Li, Y.L. Li, S.K. Wang, Z.Y. Shen, Ultimate load-carrying capacity of cold-formed thin-walled columns with built-up box and I section under axial compression, Thin Wall Struct 79, 2014.

[17] D.K. Phan, K.J.R. Rasmussen, Flexural rigidity of cold-formed steel built-up members, Thin Wall Struct 140, 2019.

[18] D.K. Phan, K.J.R. Rasmussen, Cold-formed steel bolted and screw-fastened connections in shear, Eighth International Conference on THIN-WALLED STRUCTURES. Lisbon, Portugal, 2018.

[19] AS/NZS 4600, Cold-Formed Steel Structures, Australian/ New Zealand Standard. Sydney, Australia 2018.